XLI CILAMCE
XLI Ibero-Latin American Congress on Computational Methods in Engineering
16-19 November, 2020 FOZ DO IGUAÇU PARANÁ – BRAZIL

Boundary Mesh-Free Model for elasticity problems

Fernando Martins[1], Amanda Araújo[1], Artur Portela[1]

[1]*PECC – Pós-Graduação em Estruturas e Construção Civil, Department of Civil and Environmental Engineering. University of Brasília, CEP 70910-900, Brasília-DF, Brazil.*
fernandofilho337@gmail.com, amanda.as96@gmail.com, a3portela@gmail.com

Abstract. The present work proposes implementing the shape forms obtained through the Moving Least Square (MLS) method in the Boundary Integral Equations, thus presenting a Boundary Mesh-Free Model (BMFM), based on the Boundary Node Method. Although based on the Boundary Integral Equations, BMFM does not require a boundary mesh to approximate the variables. In the proposed BMFM, the boundary is described by linear segments of integration. Within each segment, the MLS is applied independently, which allows for better representation of discontinuities on the displacement and force fields. At the end of the paper, BMFM was applied to a benchmark problem. It was possible to verify that the proposed method led to results with very low errors, proving it to be a valid alternative to the more classical, robust methods.

Keywords: Boundary Mesh-Free Model, Mesh-free Method, Elasticity, Structural Analysis.

1 Introduction

Due to the high complexity of the structures in the civil engineering field, it is not always possible to obtain the strains and stresses along the structure analytically. To overcome this problem, numerical methods, which involve some form of modelling, are usually applied, since they lead to reliable approximate results. Currently, the most popular numerical method applied is the Finite Element Method (FEM). However, FEM presents some limitations, such as: difficulty dealing with geometric nonlinear problems; considerable loss of accuracy of the stresses when a C^0 continuity is used in the interface of the elements; fracture propagation analysis; difficult implementation of adaptive meshes in three-dimensional problems. Furthermore, the generation of the mesh has a high computational cost, as presented by Andújar et al. [1], Oliveira Jr. [2] and Oliveira et al. [3].

As an alternative to FEM, it is possible to use the Boundary Element Method (BEM), which consists in discretizing only the boundary of the structure, therefore reducing considerably the use of the mesh. BEM is based on using the fundamental solutions of the differential equations, parallel to the weighted residual technique, to derive the boundary integral equation. Given the known displacements and tractions forces on the boundary, this equation describes the displacements of any point of the body. According to Brebbia and Trevelyan [4], BEM leads to better results than FEM when applied to problems with stress concentrations. It also allows for easier modeling of infinite domains. However, the generation of the mesh, even though simpler than in FEM, still presents a considerable computational cost, especially in three-dimensional problems, in which surface elements are used.

Seeking to diminish the need of mesh even further, a new class of methods, called Mesh-free or Meshless, started to be developed. This class of methods is based on the discretization of the structure through a random distribution of nodes on its boundary and/or the domain. Simply put, no pre-established connection is required between the nodes in order to approximate the variables. Mesh-free methods present better results of stress recovery and make modelling adaptive problems easier, since it is only necessary to change the position of nodes, without restrictions of position or of displacements, which is not possible when using FEM.

Thus, aiming to obtain both the benefits of the boundary integral equation, which requires that only the boundary is discretized, and of the Meshless methods, which do not require a mesh for the approximation of variables, this work proposes the implementation of the shape functions of the Moving Least Squares (MLS) on the boundary integral equations, therefore creating a new Boundary Mesh-Free Model (BMFM). At the end of the work, BMFM was applied to a benchmark problem in order for its effectiveness to be assessed.

2 Moving Least Squares

The Moving Least Squares (MLS) method is an approximation tool commonly used in Mesh-free methods for the generation of the shape functions. It is based on three components: a complete set of polynomial basis functions, a set of coefficients that are function of the space coordinates and a weight function of compact support associated with each node, as presented by Atluri and Zhu [5].

2.1 MLS approximation

The MLS approximation for $u^h(\boldsymbol{x})$ for any point on a domain is given by

$$u^h(\boldsymbol{x}) = \sum_{i=1}^{n} p_i(\boldsymbol{x}) a_i(\boldsymbol{x}) = \boldsymbol{p^T}(\boldsymbol{x})\boldsymbol{a}(\boldsymbol{x}), \tag{1}$$

in which $\boldsymbol{a}(\boldsymbol{x})$ is the vector of unknown coefficients that are functions of the space coordinates and $\boldsymbol{p^T}(\boldsymbol{x})$ is a vector of the complete monomial basis of order m.

2.2 Weight functions

The weight function $w_i(\boldsymbol{x})$ used to ponder the influence of each node based on the distance to a node i for the unidimensional case is given by a quartic spline weight function, described as

$$w_i(\boldsymbol{x}) = \begin{cases} 1 - 6\left(\frac{d_i}{r_i}\right)^2 + 8\left(\frac{d_i}{r_i}\right)^3 - 3\left(\frac{d_i}{r_i}\right)^4 & 0 \leq d_i \leq r_i \\ 0 & \text{otherwise} \end{cases}, \tag{2}$$

in which $d_i = \|x - x_i\|$ is the distance between the coordinates $\boldsymbol{x} = [x, y]$ and the node $\boldsymbol{x_i} = [x_i, y_i]$. The parameter r_i is the size of the compact support of the weight function, defined as a dimensionless parameter α_s multiplied by the greatest distance between neighbouring nodes. The compact support of a node is defined as the region in which $|w_i(\boldsymbol{x}) > 0|$. The nodes whose compact support include the node i are the ones which participate on the MLS approximation at the coordinate $\boldsymbol{x_i}$ and form what is known as the definition domain of the node i.

2.3 Shape functions

The vector $\boldsymbol{a}(\boldsymbol{x})$ of eq. (1) is determined by minimizing the J(x) norm with respect to each term of $\boldsymbol{a}(\boldsymbol{x})$, leading to

$$J(\boldsymbol{x}) = \frac{1}{2}\sum_{i=1}^{n} w_i(\boldsymbol{x})[u^h(\boldsymbol{x}) - \hat{u}_i]^2 = \frac{1}{2}\sum_{i=1}^{n} w_i(\boldsymbol{x})[\boldsymbol{p^T}(\boldsymbol{x_i})\boldsymbol{a}(\boldsymbol{x}) - \hat{u}_i]^2, \tag{3}$$

in which $\hat{u}_i$ is the nodal parameter associated with the node i. The minimization of eq. (3) leads to

$$\boldsymbol{A}(\boldsymbol{x})\boldsymbol{a}(\boldsymbol{x}) = \boldsymbol{B}(\boldsymbol{x})\hat{\boldsymbol{u}}, \tag{4}$$

in which

$$\boldsymbol{A}(\boldsymbol{x}) = \sum_{i=1}^{n} w_i(\boldsymbol{x})\boldsymbol{p}(\boldsymbol{x})\boldsymbol{p^T}(\boldsymbol{x}), \tag{5}$$

$$\boldsymbol{B}(\boldsymbol{x}) = [w_1(\boldsymbol{x})\boldsymbol{p}(\boldsymbol{x}_1), w_2(\boldsymbol{x})\boldsymbol{p}(\boldsymbol{x}_2), ..., w_n(\boldsymbol{x})\boldsymbol{p}(\boldsymbol{x}_n)], \tag{6}$$

$$\hat{\boldsymbol{u}} = [\hat{u}_1, \hat{u}_2, ..., \hat{u}_n]. \tag{7}$$

Solving eq. (4) for $\boldsymbol{a}(\boldsymbol{x})$ yields

$$\boldsymbol{a}(\boldsymbol{x}) = \boldsymbol{A}^{-1}(\boldsymbol{x})\boldsymbol{B}(\boldsymbol{x})\hat{\boldsymbol{u}}. \tag{8}$$

The shape functions $\phi_i(\boldsymbol{x})$ can then be written as

$$\phi_i(\boldsymbol{x}) = \sum_{j=1}^{m} p_j(\boldsymbol{x})[\boldsymbol{A}^{-1}(\boldsymbol{x})\boldsymbol{B}(\boldsymbol{x})]_{ji}. \tag{9}$$

Finally, the approximation functions of the MLS are rewritten as

$$u^h(\boldsymbol{x}) = \sum_{i=1}^{n} \phi_i(\boldsymbol{x})\hat{u}_i. \tag{10}$$

To insure a well-defined approximation, it is necessary that n $\geq$ m for any coordinate $\boldsymbol{x}$. Also, it is important to notice that the MLS approximations are not nodal interpolants, which means that $\phi_i(\boldsymbol{x}) \neq \delta_{ij}$.

3 Boundary Integral Equations

3.1 Fundamental solution

The fundamental solution of the elastic field in continuum domains is the solution of Kelvin's problem, that is obtaining the displacements and traction forces in any point of an infinite domain with homogenous properties, due to the action of a unitary concentrated load. For a two-dimensional problem in plane strain condition, the fundamental solution of the elastic field can be written as

$$u^*_{lk} = \frac{1}{8\pi\mu(1-\upsilon)}\left[(3-4\upsilon)ln\left(\frac{1}{r}\right)\delta_{lk} + \frac{\partial \boldsymbol{r}}{\partial \boldsymbol{x_l}}\frac{\partial \boldsymbol{r}}{\partial \boldsymbol{x_k}}\right], \tag{11}$$

in which u^*_{lk} is the displacement at any point in the k direction when a unit load is applied at i in the l direction; μ is the shear modulus; υ is Poisson's ratio; r is the distance between i and any point; x_l is the unitary vector in the l direction and δ_{lk} is the Kronecker delta.

Applying the constitutive relations of the material in eq. (11), the traction forces are found as

$$p^*_{lk} = \frac{-1}{4\pi(1-\upsilon)r}\left[\left[\frac{\partial \boldsymbol{r}}{\partial \boldsymbol{n}}(1-2\upsilon)\,\delta_{lk} + 2\frac{\partial \boldsymbol{r}}{\partial \boldsymbol{x_l}}\frac{\partial \boldsymbol{r}}{\partial \boldsymbol{x_k}}\right] + (1-2\upsilon)\left(n_l\frac{\partial \boldsymbol{r}}{\partial \boldsymbol{x_k}} - n_k\frac{\partial \boldsymbol{r}}{\partial \boldsymbol{x_l}}\right)\right], \tag{12}$$

in which p^*_{lk} is the traction force at any point in the k direction when a unit load is applied at i in the l direction and $\boldsymbol{n}$ is the normal vector to the surface of the domain.

3.2 Somigliana Boundary Integral Equations

Consider the static equilibrium equation, eq. (13), with a set of constrained displacements, eq. (14), and a system of external forces, eq. (15):

$$\sigma_{kj,k} + b_k = 0, \tag{13}$$

$$u_k = \bar{u}_k \ \text{ on the boundary } \Gamma_u, \tag{14}$$

$$p_k = \sigma_{kj}n_j = \bar{p}_k \ \text{ on the boundary } \Gamma_t, \tag{15}$$

in which $\sigma_{kj,j}$ are the stress components, b_k are the body force components, n_j are the normal vector components, p_k are the traction force components, u_k are the displacement components, $(\bar{\cdot})$ represent prescribed or known values, and $\Gamma = \Gamma_u + \Gamma_t$ is the complete boundary of the domain. Applying the weighted residual method to eq. (13) and considering the fundamental solution as the weight leads to:

$$\int_\Omega \left(\sigma_{kj,j} + b_k\right) u^*_{lk} d\Omega = 0. \tag{16}$$

Integrating eq. (16) twice by parts and using both the constitutive relations of the material and the properties of the fundamental solution, the Somigliana integral is obtained as:

$$u^i_k + \int_\Gamma p^*_{lk} u_k d\Gamma = \int_\Gamma u^*_{lk} p_k d\Gamma + \int_\Omega u^*_{lk} b_k d\Gamma. \tag{17}$$

Using eq. (17), it is possible to determine the displacement of any internal point i knowing only the traction and body forces, the fundamental solution of the elastic field and the boundary constraints u_k and p_k. When the source point is on the boundary, eq. (17) leads to:

$$c^i_{lk} u^i_k + \int_\Gamma p^*_{lk} u_k d\Gamma = \int_\Gamma u^*_{lk} p_k d\Gamma + \int_\Omega u^*_{lk} b_k d\Gamma. \tag{18}$$

in which c^i_{lk} is a constant. The analytical determination of c^i_{lk} can be complicated, but its value can be easily obtained using rigid body considerations, demonstrated in Brebbia and Dominguez [6].

4 Boundary Mesh-Free Model

This chapter introduces the proposed formulation for the Boundary Mesh-Free Model (BMFM), which is based on the Boundary Node Method (BNM), presented by Kothnur et al. [7]. Both methods apply the MLS shape functions on the Boundary Integral Equations. However, they differ in the way the final system of equations is solved; the weight function; and the way in which the MLS is applied, since in the BNM the MLS is applied on the entire boundary as a whole, while on the BMFM it is applied separately in each segment of integration, thus allowing for a better representation of discontinuities on the variable fields.

Firstly, consider that the boundary Γ of a two-dimensional body is divided in N linear segments of integration Γ_j. Each Γ_j segment is discretized with an arbitrary set of nodes n_j linked by linear sub-segments, as represented in Fig. 1. The end segments, shared by pairs of contiguous Γ_j segments, can either contain nodes or not. On each boundary segment Γ_j, the MLS is applied independently for the approximation of the displacements, eq. (19), and traction forces, eq. (20).

$$\boldsymbol{u} = \boldsymbol{\Phi}_j \hat{\boldsymbol{u}}^j, \tag{19}$$

$$\boldsymbol{p} = \boldsymbol{\Phi}_j \hat{\boldsymbol{p}}^j, \tag{20}$$

in which $\hat{\boldsymbol{u}}^{\boldsymbol{j}}$ e $\hat{\boldsymbol{p}}^{\boldsymbol{j}}$ are, respectively, the displacement and the traction force parameters of the n_j nodes of the segment Γ_j; $\boldsymbol{u}$ and $\boldsymbol{p}$ are vectors, each composed of two components and represent the displacements and traction forces of any point within the segment Γ_j; and $\boldsymbol{\Phi}_j$ is the matrix of shape functions, of the order 2x2n_j, of nodes included in the definition domain of the field point $\boldsymbol{x}$, expanded with zero entries for remaining nodes of the segment. The body forces can also be represented as a vector of two components $\boldsymbol{b}$. Finally, $\boldsymbol{u^*}$ and $\boldsymbol{p^*}$ represent the 2x2 matrix of the fundamental solution and its derivative.

Hence, given the discretization of the boundary in N linear segments of integration and of the domain in M internal cells (necessary in problems in which there are body forces acting), and considering the MLS approximation, eq. (18) can be rewritten as:

$$\boldsymbol{c}^i \boldsymbol{\Phi}^i_j \hat{\boldsymbol{u}}^j + \sum_{j=1}^{N} \int_{\Gamma_j} \boldsymbol{p^*} \boldsymbol{\Phi}_j d\Gamma \hat{\boldsymbol{u}}^j = \sum_{j=1}^{N} \int_{\Gamma_j} \boldsymbol{u^*} \boldsymbol{\Phi}_j d\Gamma \hat{\boldsymbol{p}}^j + \sum_{s=1}^{M} \int_{\Omega_s} \boldsymbol{u^*} \boldsymbol{b} d\Omega \ \text{ or} \tag{21}$$

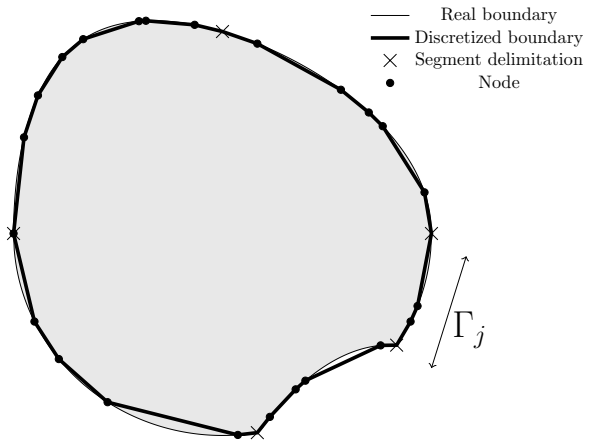

Figure 1. BMFM discretization of the boundary Γ, defined with N segments Γ_j

$$(\boldsymbol{C}^i + \boldsymbol{H}^i)\hat{\boldsymbol{U}} = \boldsymbol{G}^i\hat{\boldsymbol{P}} + \boldsymbol{B}^i, \tag{22}$$

in which

$$\boldsymbol{H}^i = \sum_{j=1}^{N} \int_{\Gamma_j} \boldsymbol{p}^* \boldsymbol{\Phi}_j d\Gamma, \tag{23}$$

$$\boldsymbol{C}^i = \boldsymbol{c}^i \boldsymbol{\Phi}_j^i, \tag{24}$$

$$\boldsymbol{G}^i = \sum_{j=1}^{N} \int_{\Gamma_j} \boldsymbol{u}^* \boldsymbol{\Phi}_j d\Gamma. \tag{25}$$

$$\boldsymbol{B}^i = \sum_{s=1}^{M} \int_{\Omega_s} \boldsymbol{u}^* \boldsymbol{b} d\Omega. \tag{26}$$

Once eq. (22) is applied to all i boundary nodes and the numerical integration (using Gaussian quadrature for nodes that are far from the singularity and the logarithmic Gaussian quadrature for those near the singularity) is finished, the global system can be arranged as

$$(\boldsymbol{C} + \boldsymbol{H})\hat{\boldsymbol{U}} = \boldsymbol{G}^i\hat{\boldsymbol{P}} + \boldsymbol{B}, \tag{27}$$

in which $\hat{\boldsymbol{U}}$ and $\hat{\boldsymbol{P}}$ represent the nodal parameters of displacement and traction force nodal of all the boundary nodes, and $\boldsymbol{H}$, $\boldsymbol{C}$ and $\boldsymbol{G}$ are the global coefficient matrixes. Since $\hat{\boldsymbol{U}}$ and $\hat{\boldsymbol{P}}$ do not represent the nodal approximation values, the imposition of boundary constraints is done by rearranging eq. (27), leading to

$$\begin{bmatrix} (\boldsymbol{C} + \boldsymbol{H}) & -\boldsymbol{G} \\ \boldsymbol{\Phi}_{\hat{\boldsymbol{U}}} & \boldsymbol{0} \\ \boldsymbol{0} & \boldsymbol{\Phi}_{\hat{\boldsymbol{P}}} \end{bmatrix} \begin{bmatrix} \hat{\boldsymbol{U}} \\ \hat{\boldsymbol{P}} \end{bmatrix} = \begin{bmatrix} \boldsymbol{B} \\ \boldsymbol{U} \\ \boldsymbol{P} \end{bmatrix} \tag{28}$$

in which $\boldsymbol{\Phi}_{\hat{\boldsymbol{U}}}$ and $\boldsymbol{\Phi}_{\hat{\boldsymbol{P}}}$ are the matrixes of the MLS shape functions of the nodes with prescribed values of body forces $\boldsymbol{B}$, displacements $\boldsymbol{U}$ and of traction forces $\boldsymbol{P}$, respectively.

Finally, the system of equations presented in eq. (28) can be solved for $\hat{\boldsymbol{U}}$ and $\hat{\boldsymbol{P}}$. Once the nodal parameters are known, it is possible to approximate $\boldsymbol{u}$ and $\boldsymbol{p}$ in any boundary point using eq. (10). Once the displacement of any internal point is obtained using the Somigliana integral, eq. (17), the stresses can be calculated using Hooke's law.

5 Numerical results

The material properties used in the benchmark were: E = 27 GPa and υ = 0.2. The BMFM results were compared to the analytical ones and the average relative error (E_m) was estimated using eq. (29). The points in which $u^i_{analytical} = 0$ were not considered in the calculation of the error.

$$E_m = \frac{1}{n}\sum_{j=1}^{N}\left|\frac{u^i_{analytical} - u^i_{BMFM}}{u^i_{analytical}}\right| \tag{29}$$

The benchmark was a plate with a circular hole under unidirectional tension of P=-30 MPa along the x direction in the plane stress state, as seen in Fig. 2a. Due to symmetry, only a portion of the upper right quadrat of the plate is considered, with b x b dimensions. The circle has a radius of a = 1, with b=5a. The analytical solutions of the problem are given by eq. (30) and eq. (31). The nodal distribution is presented in Fig. 2b. The discretization consisted in 51 nodes. The ends of all the segments, represented by an x, have two nodes, one belonging to each neighbouring segment. A quadratic polynomial base was used (m=3) and α_s = 3.7. The numerical results are presented in Fig. 3 for the displacements and Fig. 4 for the stresses. It is clear by the graphs and their E_m errors that the BMFM obtained results extremely close to the analytical ones.

$$\begin{cases} u_x(r,\theta) = \frac{1+\upsilon}{E}P\left(\frac{rcos}{1+\upsilon} + \frac{2}{1+\upsilon}\frac{a^2}{r}cos\theta + \frac{1}{2}\frac{a^2}{r}cos3\theta - \frac{1}{2}\frac{a^4}{r^3}cos3\theta\right) \\ u_y(r,\theta) = \frac{1+\upsilon}{E}P\left(\frac{-\upsilon}{1+\upsilon}rsin\theta - \frac{1-\upsilon}{1+\upsilon}\frac{a^2}{r}sin\theta + \frac{1}{2}\frac{a^2}{r}sin3\theta - \frac{1}{2}\frac{a^4}{r^3}sin3\theta\right) \end{cases}, \tag{30}$$

$$\begin{cases} \sigma_{xx}(r,\theta) = P\left[1 - \frac{a^2}{r^2}\left(\frac{3}{2}cos2\theta + cos4\theta\right) + \frac{3}{2}\frac{a^4}{r^4}cos4\theta\right] \\ \sigma_{yy}(r,\theta) = P\left[-\frac{a^2}{r^2}\left(\frac{1}{2}cos2\theta - cos4\theta\right) - \frac{3}{2}\frac{a^4}{r^4}cos4\theta\right] \\ \sigma_{xy}(r,\theta) = P\left[-\frac{a^2}{r^2}\left(\frac{1}{2}sin2\theta - sin4\theta\right) + \frac{3}{2}\frac{a^4}{r^4}sin4\theta\right] \end{cases}. \tag{31}$$

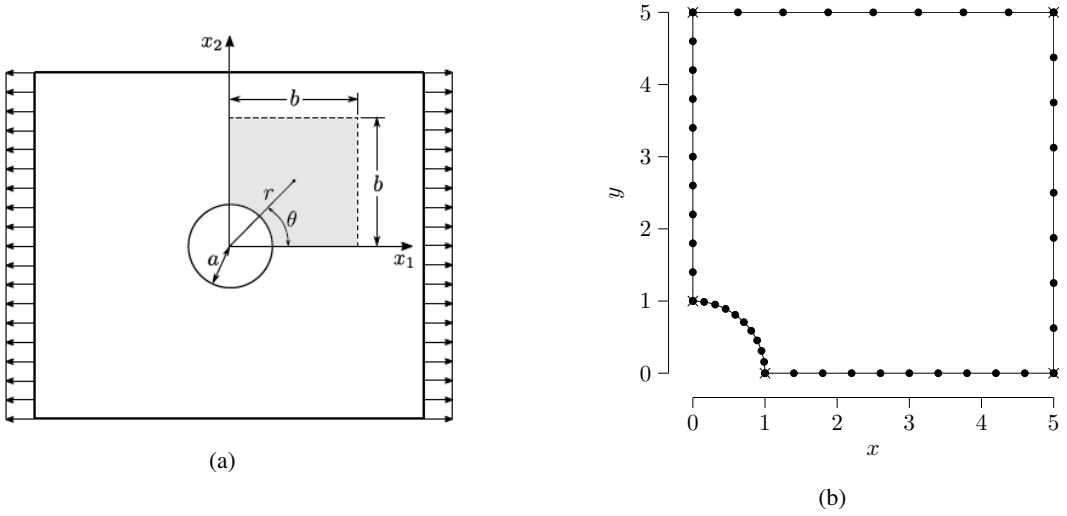

(a) (b)

Figure 2. (a) Plate with a circular hole. Source: Oliveira Jr. [2] (b) BMFM discretization of the problem

6 Conclusions

The present work proposed a Boundary Mesh-Free Model (BMFM), which combines the advantages of the Mesh-free methods (of not needing any sort of connectivity between nodes in order to approximate the variables) and of the Boundary Integral Equations (of only requiring a discretization of the boundary), while using the shape forms generated by the Moving Least Squares method. The proposed formulation was then applied to a benchmark problem. In all cases, the BMFM approximation lead to small errors when compared to the analytical results, thus

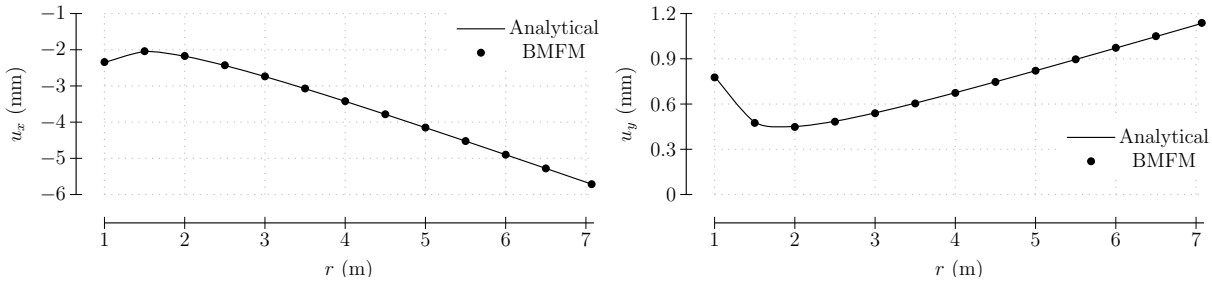

(a) (b)

Figure 3. Displacements at $\theta = 45^{\text{o}}$ (a) U_x, E_m =0.20% (b) U_y, E_m =0.40%

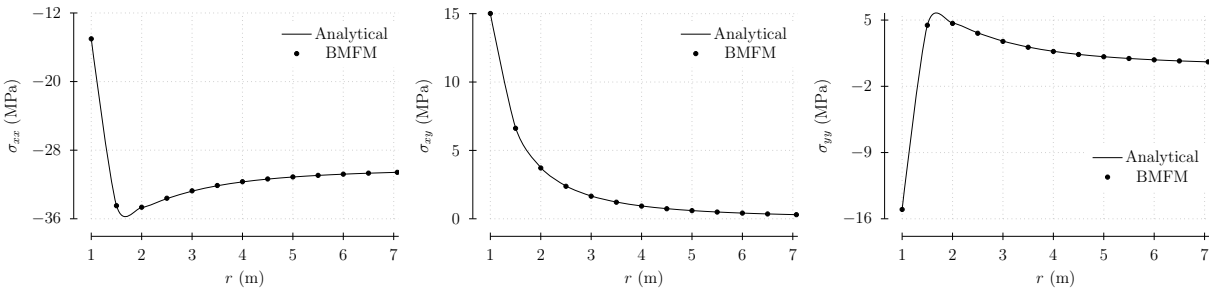

(a) (b) (c)

Figure 4. Stresses at $\theta = 45^{\text{o}}$ (a) σ_{xx}, E_m=0.06% (b) σ_{xy}, E_m =0.70% (c) σ_{yy}, E_m =0.60%

proving its effectiveness. Therefore, it is clear that the BMFM presented here can be a reliable alternative to the classic numerical method applied nowadays in elasticity problems.

Acknowledgements. The authors of this paper acknowledge the financial support given by CAPES.

Authorship statement. The authors hereby confirm that they are the sole liable persons responsible for the authorship of this work, and that all material that has been herein included as part of the present paper is either the property (and authorship) of the authors, or has the permission of the owners to be included here.

References

[1] Andújar, R., Jaume, R., & Vojko, K., 2011. Beyond fem: overview on physics simulation tools for structural engineers. *Technics Technologies Education Management*, vol. 6.3, pp. 555–571.

[2] Oliveira Jr., V. G., 2015. *Formulação cinemática local de métodos sem malha*. Masters dissertation, Departamento de Engenharia Civil e Ambiental, Universidade de Brasília.

[3] Oliveira, T., Vélez, W., Santana, E., Araújo, T., Mendonça, A., & PORTELA, A., 2019. A local mesh free method for linear elasticity and fracture mechanics. *Engineering Analysis with Boundary Elements*, vol. 101, pp. 221–242.

[4] Brebbia, C. & Trevelyan, J., 1986. On the accuracy and convergence of boundary element results for the floyd pressure vessel problem. *Computers Structures*, vol. 24, pp. 513–516.

[5] Atluri, S. & Zhu, T., 2000. New concepts in meshless methods. *International Journal for Numerical Methods in Engineering*, vol. 47, pp. 537–556.

[6] Brebbia, C. & Dominguez, J., 1992. *Boundary Elements An Introductory Course, 2nd Ed.* WIT Press, Ashurst Lodge, UK.

[7] Kothnur, V., Mukherjee, S., & Mukherjee, Y., 1999. Two-dimensional linear elasticity by the boundary node method. *International Journal of Solids and Structures*, vol. 36, pp. 1129–1147.